PHILOSOPHICAL TRANSACTIONS OF THE ROYAL SOCIETY A MATHEMATICAL, PHYSICAL & ENGINEERING SCIENCES

New Developments in Measurement Techniques for High Temperature Plasmas

N. J. Peacock and D. D. Burgess

Phil. Trans. R. Soc. Lond. A 1981 **300**, 665-682
doi: 10.1098/rsta.1981.0094

Phil. Trans. R. Soc. Lond. A **300**, 665–682 (1981) [665]
Printed in Great Britain

New developments in measurement techniques for high temperature plasmas

By N. J. Peacock† and D. D. Burgess‡
† *Euratom./U.K.A.E.A. Fusion Association, Culham Laboratory, Abingdon, Oxfordshire OX*14 3*DB, U.K.*
‡ *Imperial College, London SW*7 2*AZ, U.K.*

This review covers topical diagnostic developments appropriate to the study of a wide range of multi-kiloelectronvolt temperature laboratory plasmas.

1. Introduction

Recent developments in measurement techniques on high temperature laboratory plasmas have been influenced by three main factors. Most important is the plasma physicists ability to generate and control an ever wider range of new, more energetic plasma conditions. Tokamaks, for instance, now provide laboratory plasmas which approximate to the most active regions of the solar corona in terms of temperature and emitter charge state; the latter ranges up to, say, $Z = 50$. At the other end of the scale, extreme pressure plasma conditions with densities comparable to those in solids are now produced in laser-irradiation experiments. At these densities many basic approximations usually assumed in diagnostic measurements, for example the binary collisional excitation model, need reconsideration.

Other new measurement techniques stem directly from advances in the technology of diagnostic apparatus such as lasers and photo-electronics. Fluorescence spectroscopy and far infra-red light scattering are but two examples.

Finally, the use of numerical methods to assemble and reduce line-of-sight data has proved very informative, as in the case of the tomographic analyses of the X-ray emission from both tokamaks and laser-compressed plasmas.

This paper briefly discusses all of these aspects of diagnostic developments, and highlights the close connection between plasma measurement techniques and the study of basic atomic or ionic processes. Appropriate surveys of diagnostic methods in modern fusion devices are to be found in the Varenna School publications (Eubank & Sindoni 1975, Sindoni & Wharton 1978), in the article by Equipe T.F.R. (1978), and by Attwood (1978) and Ahlstrom *et al.* (1978).

2. Plasma parameters in state-of-the-art fusion devices

The range of parameters describing laboratory plasmas has increased dramatically over the last few years due largely to the pursuance of controlled fusion research. In tokamak plasmas, operating over an electron density range $5 \times 10^{18} \lesssim n_e \lesssim 5 \times 10^{20}$ m^{-3}, multi-kiloelectronvolt temperatures, are now routinely produced by ohmic heating (Bol *et al.* 1979). Neutral particle beam injection at the megawatt level can raise the ions to equivalently high temperatures (Eubank *et al.* 1979). Owing partly to the larger plasma volumes (of the order of cubic metres) in current tokamaks, these temperatures are not achieved at the expense of impaired plasma containment, the product of density and particle confinement time being typically

$n_e\tau \gtrsim 10^{18}\,\mathrm{m^{-3}\,s}$. These parameters have important consequences for measurement techniques associated with the X-ray emission from highly charged ions which are often present as impurities in a background plasma of ionized hydrogen or its isotopes. The large $n\tau$ value makes possible measurements with simultaneous high spatial and spectral resolution while the relatively low n_e allows observations of optically forbidden transitions, (§5.3).

In high energy density plasmas such as those produced from solids by laser heating and compression, multi-kiloelectronvolt temperatures have also been achieved, albeit on a sub-nanosecond time scale and in minute, $10^{-15}\,\mathrm{m^3}$ plasma volumes (Attwood *et al.* 1979, Ceglio & Coleman 1977). The inertial confinement factor (equivalent to $n_e\tau$ for magnetic confinement) is $\int \rho\,\mathrm{d}r \approx 10^{-2}\,\mathrm{kg\,m^{-2}}$ and this parameter together with the electron temperature determines the ionization state in these compressed plasmas which have densities typically in the range $10^{25} \leqslant n_e < 10^{30}\,\mathrm{m^{-3}}$. An important diagnostic technique here again involves high-Z emitters since detailed emission line shapes can be interpreted directly in terms of the parameters $\int \rho\,\mathrm{d}r$ and the density ρ, §5.4.

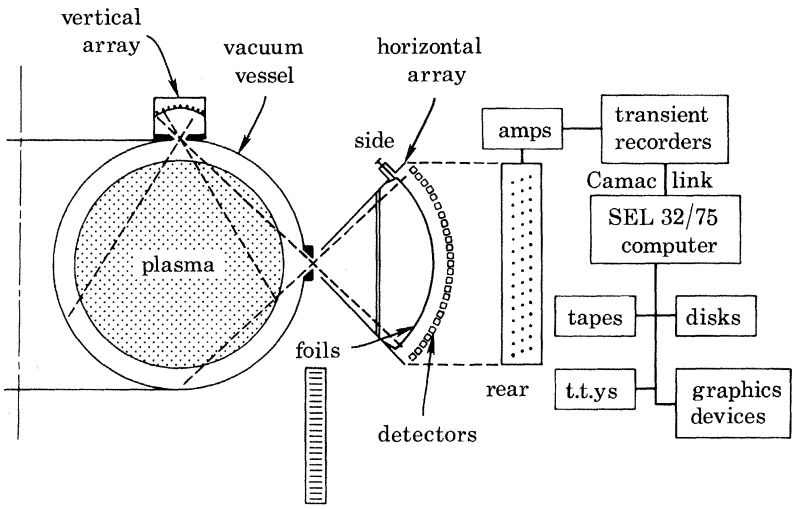

FIGURE 1. Schematic layout of X-ray detectors and signal retrieval system used for tomographic analyses of X-ray emission (1 keV $\lesssim h\nu \lesssim$ 13 keV) from tokamaks at the Princeton Plasma Physics Laboratory (t.t.ys: telytypes). The surface barrier detectors (typically twenty in an array) view chordal line-of-sight intensities from the plasma and have a linear response up to 1 MHz frequency (Sauthoff *et al.* 1978).

3. DATA RETRIEVAL: DERIVATION OF LOCAL PARAMETERS BY METHODS OF RECONSTRUCTION

3.1. *X-ray tomography*

Modern data-gathering techniques, with their ability to handle and cross-correlate many data points taken at a single time make practical the derivation of local parameters that previously were unobtainable. For example, the derivation of local quantities from their line-of-sight integrals finds an important application in the study of the spatial plasma profiles in high temperature tokamaks, line-of-sight, chordal X-ray emission being used as the basic data (Sauthoff *et al.* 1978).

The X-ray emission along a number of chords, typically twenty, is viewed by an array of surface barrier detectors, figure 1, each array monitoring various poloidal and toroidal

positions about the torus. Because of the degree of cylindrical symmetry and the often uniform periodic nature of the instability signals in tokamaks, the X-ray intensities can be interpreted to a large degree in terms of the motion of rigid plasma rotators. The rotation of the $m = 2$ poloidal mode and its growth rate is most readily understood on this model and is illustrated in figure 2. Non-uniform rotation and high m (poloidal) and n (toroidal) disturbances require more complicated analyses of numerous measurements, some along the toroidal field lines.

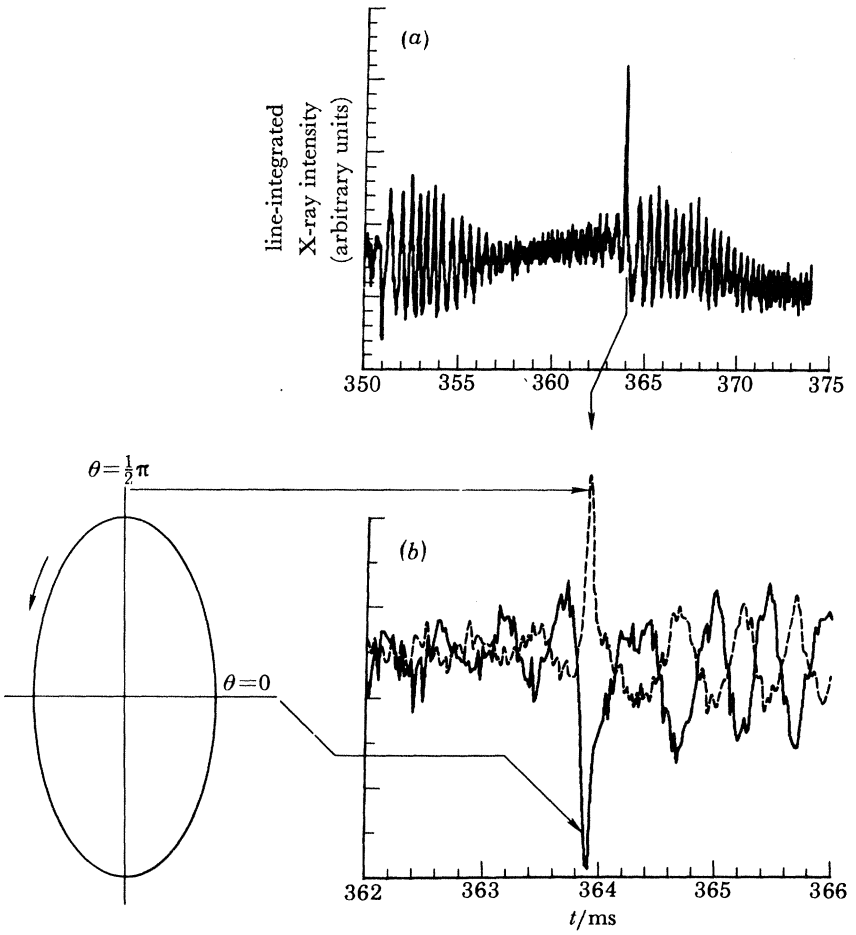

FIGURE 2. (*a*) Central, chordal X-ray intensity in the horizontal plane illustrating two bursts of m.h.d. activity in the P.L.T. tokamak, one at 350 ms, the other at 364 ms. If the plasma is a rigid rotator, the poloidal harmonics generate frequency components due to Doppler shifts, the frequency being proportional to the mode number in the direction of rotation. (*b*) Superimposition of central chord traces from views rotated by 90°. The growth of the $m = 2$ component is seen (Bol *et al.* 1979).

Much of the instability information can be derived purely in terms of the X-ray intensity isocontours without recourse to their detailed interpretation in terms of δn_e and δT_e. This detailed information, however, can be derived from simultaneous measurements of the far infra-red emission at the electron and cyclotron frequencies, see §3.2.

A quite different approach to tomographic analysis is required to unfold the spatial variation of the particle and photon emission produced in laser compression experiments of microspheres. These minute, high pressure (less than about 10^8 atm $\approx 10^{13}$ Pa) plasmas have

dimensions $r \approx 100$ μm and require spatial resolution $\delta r \approx 1$ μm. At the Livermore Laboratory Ceglio and co-workers (Ceglio *et al.* 1977; Ceglio & Coleman 1977; Ceglio & Smith 1978) use coded aperture imaging techniques. This imaging technique as applied to X-ray microscopy is a two-step process. In the first step, diffraction plays no part and radiation from the source casts a simple shadow of the coded aperture onto a suitable detector plane which may be photographic emulsion, cellulose nitrate film (for α-particles) or a solid state detector array. The use of Fresnel zones as the coded aperture makes the second step particularly simple since visible lasers can be used to illuminate the shadowgraph transparency and, as in holography, reconstruct a three-dimensional image of the original source. Ceglio and co-workers, using micro-Fresnel-zone plates made from 5–10 μm gold foil with a few hundred zones, typically achieve a radial plasma resolution δr of the order of a micrometre with tomographic (in depth) resolutions of some tens of micrometres.

3.2. *Emission at or near the plasma frequency and the cyclotron frequency*

An interesting example of how increases in plasma containment time, volume, temperature, etc. can sharply change the technological requirements for a successful diagnostic technique is the recent re-emergence of far infrared (f.i.r.) emission spectroscopy as a powerful means of obtaining diagnostic information, in many cases spatially resolved (Costley 1979). After the pioneering work on time-resolved pulsed Fourier transform spectroscopy of transient plasma done jointly by Imperial College and N.P.L. (Chamberlain *et al.* 1971) the use of this technique on tokamaks by Costley and his collaborators, together with alternative f.i.r. dispersion methods used by other groups have shown how powerful f.i.r. emission measurements can be when applied to a long-lived, high temperature, relatively low density magnetized plasma, and in particular to plasmas where $\omega_{\mathrm{c.e.}}$, the electron cyclotron frequency, exceeds $\omega_{\mathrm{p.e.}}$, the plasma frequency.

The success of this technique in providing spatially resolved information, for example on electron temperatures in tokamaks, depends on the fact that the radial variation of magnetic field strength, and hence of the electron cyclotron frequency and its harmonics, is essentially known *a priori*. A study of the spectral structure of the emission near each harmonic therefore reflects the spatial variation of the plasma parameters and can be interpreted to yield a unique value for a radial variation of T_{e} if the harmonic is optically thick, and of electron density, n_{e}, if the harmonic is optically thin. Figure 3 shows an example of the emission spectrum from the DITE tokamak. The intensity variation through the optically thick second harmonic is directly related to a saddle-shaped $T_{\mathrm{e}}(r)$ profile in the tokamak. This technique has the advantage over Thomson scattering that by using only a single detector it is possible to obtain a more-or-less continuous monitor of the radial variation of T_{e} and n_{e} during a single plasma shot, since the spectrum will usually contain both optically thick and optically thin harmonics. The capability of the f.i.r. diagnostic is well illustrated in figure 4 by the continuous electron temperature profile scans of a neutral beam heated plasma in the P.L.T. tokamak. The interval between profile scans in this instance is *ca.* 10 ms but with further immediate developments resolution intervals of *ca.* 1 ms are anticipated.

In principle, observations of emission at $\omega_{\mathrm{p.e.}}$, and of the polarization of the emission at $\omega_{\mathrm{c.e.}}$, can provide further information. The polarization properties are of particular importance, since they can provide information on the variation of magnetic field pitch angle with field strength and hence position. However, several measurements, particularly early ones, failed to show any of the expected polarization of $\omega_{\mathrm{c.e.}}$ and its harmonics (Costley *et al.* 1974) and the

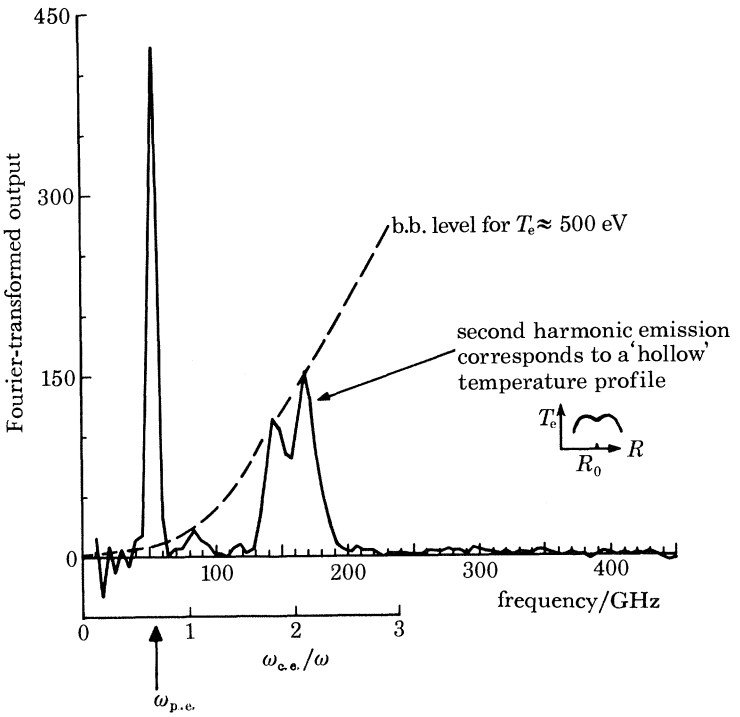

FIGURE 3. Fourier-transformed spectrum of the f.i.r. emission from the DITE tokamak showing a suprathermal emission at $\omega_{p.e.}$ and the optically thick features at $\omega_{c.e.}$ and $2\omega_{c.e.}$ compared with the black-body emission (b.b.) at the free electron temperature $T_e \approx 500$ eV. From the detailed shape of the $2\omega_{c.e.}$ harmonic, a 'hollow' radial temperature profile is derived. (Courtesy of A. E. Costley (N.P.L.) and the DITE group, Culham Laboratory.)

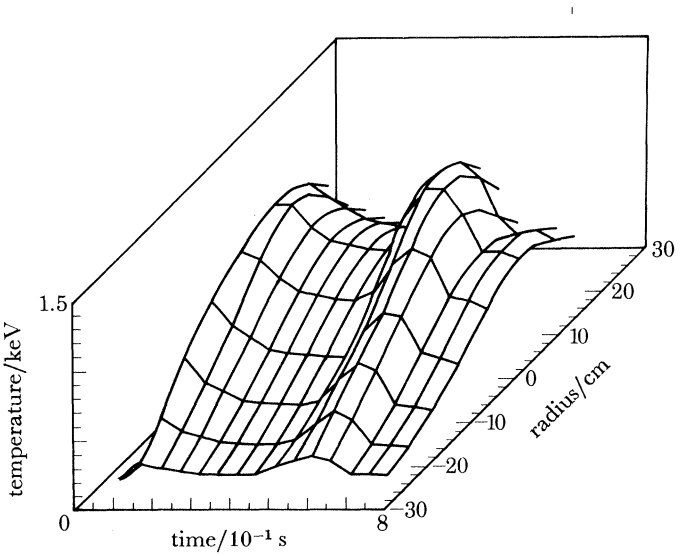

FIGURE 4. Temperature profile in the P.L.T. tokamak derived from Fourier transform spectroscopy of the optically thick cyclotron emission. (Courtesy of D. A. Boyd (University of Maryland) and Princeton Plasma Physics Laboratory.)

expected dominance of the E-mode over the O-mode was not observed (Costley *et al.* 1977). These discrepancies now appear to have been resolved as an effect of polarization scrambling of the radiation which can be multiply scattered from the walls of the plasma chamber before reaching the detector.

Attention has also been given to the effect of runaway electrons on emission at the electron plasma frequency, $\omega_{\text{p.e.}}$ (Hutchinson *et al.* 1977; Freund *et al.* 1978), which in appropriate circumstances can greatly exceed the black-body level. The spectrum of the DITE tokamak, figure 3, clearly shows both structure in the first harmonic of $\omega_{\text{c.e.}}$, and greatly enhanced emission at $\omega_{\text{p.e.}}$. In extreme cases it has been found that the spectrum is dominated by runaway electrons, the cyclotron frequency harmonics appearing as absorption dips rather than peaks.

Major differences in the appearance of the spectra will arise in the new generation of tokamaks such as JET. These differences arise because of relativistic effects, because of the high opacity and because emission from the separate harmonics will largely overlap when viewed along the major radius of the torus. The recorded spectrum, although expected to be somewhat featureless, in contrast to that shown in figure 3, will still carry enough information for n_{e}, T_{e}, the poloidal field, B_{P}, and the runaway level to be derived on a single-shot basis.

4. Diagnostics based on photon scattering

4.1. *Use of fixed-frequency lasers*

In those plasmas where $\omega_{\text{p.e.}}$ is less than the output frequency of contemporary high power lasers, Thomson scattering has become a routine technique for probing the internal structure of the plasma.

The interpretation of the complicated spectral density function $S(\omega, k)$ of the scattered light, in terms of the various collective and independent motions of the particles, has been treated fully in texts (Sheffield 1975), and in review articles (e.g. Evans & Katzenstein 1969; Evans 1976*a*; 1977). It suffices here to note that scattering from the collective motion of the electrons, such as plasma waves or 'dressed' ion motion, occurs when the scattering length, $k^{-1} = c/2\omega_0 \sin \frac{1}{2}\theta$, is equal to or exceeds the Debye length, i.e. $\alpha \equiv (k\lambda_{\text{D}})^{-1} \gtrsim 1$. For visible light scattering from low density and high temperature plasmas, for example tokamaks, $\alpha \equiv (k\lambda_{\text{D}})^{-1} \ll 1$ and the scattered light spectrum $S(\omega, k)$ is determined by the random thermal fluctuations of the electrons. The incoherent spectral density function is then routinely used to derive the electron velocity distribution, the main complications being current-driven electron drifts and relativistic corrections which at elevated temperatures, $T_{\text{e}} \gtrsim 5$ keV, can cause pronounced skewing of the spectrum to the blue side.

The development of scattering as a diagnostic in recent years, however, has been aimed at collective effects in high temperature tokamaks. Practical difficulties arise from the long scale length (k^{-1}) which has to be probed. Infrared (i.r.), even far infrared (f.i.r.) lasers, or very small scattering angles, θ, or a combination of both are required. In contrast to visible light scattering where the scattered signal/noise ratio is set by plasma background emission, the main problem in the f.i.r. region is detector noise. F.i.r. lasers themselves have only recently been developed with sufficient brightness and power (more than 10 kw) to be of use for scattering at reasonable scattering angles, $\theta \gtrsim 10°$ say. Despite a fair amount of technological development (see, for example, Evans 1977; Luhmann 1979), no successful i.r. or f.i.r.

scattering experiments on tokamaks have yet been reported for such collective ion features as ion-thermal motion, highly charged ion enhancement and ion cyclotron modulation.

A notable exception to this somewhat slow progress has been the very small scattering angle experiments by Slusher & Surko (1980). These authors have successfully used a single-mode CW CO_2-laser, operating in the i.r. at 10 μm with a modest output of about 100 W, to probe *supra-thermal* density fluctuations with wavelengths in the range 0.01–1 cm in tokamak plasmas. The frequency shifts due to these fluctuations are typically 10^3–10^{10} Hz. The scattering angle in these experiments is so small as to be almost within the probe beam divergence, and heterodyne mixing of the optical signals from the scattered light and a local oscillator takes place within a photoconductive (for example, liquid He-cooled, Sb-doped Ge:Cu) detector. The detector signal, processed by a spectrum analyser, directly gives $S(\omega, k)$ due to the density fluctuations. The inherently poor spatial resolution of forward scattering is obviated by searching for correlation frequencies in the forward scattered light from two intersecting probe beams. Two-dimensional isotropic turbulence and $m = 2$ instability-driven turbulence have been observed by Slusher & Surko (1980). However, perhaps their most interesting observation is that the volume-distributed turbulence observed near the lower operating range of density in tokamaks changes to surface turbulence in more collisional, higher density plasmas. Collective scattering measurements on *quiescent* low density tokamak conditions require considerably higher CO_2 laser peak powers, typically more than about 10 kW, and such experiments are now being attempted at the Princeton Plasma Physics Laboratory and elsewhere.

Another noteworthy advance has been the 'proof-in-principle' measurements of the pitch angle of the magnetic field lines in tokamaks by using light scattering Forrest *et al.* (1978). The extreme sensitivity of the cyclotron modulation in the scattered visible light spectrum to the angle between the local field direction and the scattering vector, $\boldsymbol{k}$, has been exploited by these authors to determine the pitch angle of the field lines to $\pm 0.15°$. Scattering from Bernstein waves due to electrons orbiting around magnetic field lines had previously been demonstrated in low temperature, higher density plasmas with $\bar{n}_e \approx 10^{22}\,\mathrm{m}^{-3}$ (Evans & Carolan 1970). At the lower densities and much higher temperatures in tokamaks, the separate cyclotron harmonics cannot be observed without recourse to optical multiplexing techniques (Forrest *et al.* 1978).

4.2. *Photon scattering using tunable lasers*

Photon scattering at or near atomic resonance frequencies in a plasma (fluorescence or Rayleigh scattering respectively) offers several possibilities complimentary to those of Thomson scattering, for example in the determination of neutral hydrogen spatial distributions, magnetic field directions, impurity concentrations and diffusion rates (Measures 1968; Burgess 1972, 1978*a*; Radzobarin *et al.* 1978; Evans 1976*b*; Dimmock *et al.* 1969; Bogen & Hintz 1978; Burakov *et al.* 1977). While a considerable number of fluorescence experiments have been reported on collisional processes in various low temperature laboratory plasmas (Burrell & Kunze 1972; Burgess & Skinner 1974; Himmel & Pinnekamp 1978; Burgess *et al.* 1978, 1980), only recently have diagnostics experiments been performed on actual fusion devices as in the experiments of Radzobarin (1978), Muller & Burrell (1980) and Schweer *et al.* (1980).

The most commonly considered technique to date has been observation of resonant fluorescence excited with tunable lasers. Resonance scattering offers effective scattering cross sections some 10^{10}–10^{14} larger than the Thomson cross section (dependent on transition, spectral line

width, etc.), and hence reduced needs on input laser power plus the possibility of observing very small species concentrations.

For saturated resonance scattering, the limitations on signal-to-background and hence spatial resolution in high temperature plasmas are primarily set by the low initial population difference between the upper and lower states of transitions accessible with current tunable laser wavelengths; this consideration has led several groups to develop tunable laser systems operating at or near Lyman-α, 121.5 nm (Mahon *et al.* 1978; Cotter 1979) and Lyman-β (Reintjes 1979). In principle the best technique for scattering from atomic hydrogen would probably be Lyman-β illumination followed by observation of the consequent Balmer-α scattering in the visible spectral region. However, this statement presumes equality of incident pulse length between u.v. and visible lasers, and currently when possible pulse lengths, and hence total scattering fluxes, are 10^2–10^3 larger for visible-frequency lasers, Balmer-α illumination is still a very serious contender. A simple, but elegant, development in this context has been the use, by Radzobarin and his co-workers on experiments on the F.T.-1 device, of optical methods allowing subtraction of Balmer-α resonance fluorescence from the strong plasma background emission (Burakov *et al.* 1977; Radzobarin & Folomkin 1978).

The maximum scattered intensity from off-resonance (Rayleigh) scattering will saturate at the same value as for the on-resonance case. However, an important potential advantage of off-resonance scattering (Evans 1976*b*; Wrobel *et al.* 1976) is that of being able to tune the scattered frequency away from strong background plasma line emission. This advantage is more significant for Doppler-broadened lines than for pressure-broadened transitions since in the latter case the scattering cross section and the emission both fall off as $\Delta\omega^{-2}$, where $\Delta\omega$ is the frequency detuning from resonance. The major limitation on Rayleigh scattering measurements is, perhaps, that in many situations the various tunable lasers commonly in current use are of inadequate power to compensate for the reduced cross-section in comparison with resonant scattering, and thus to overcome the Bremsstrahlung background. A further limitation is that the potential for avoiding background line emission by detuning is severely limited, since due to the $\Delta\omega^{-2}$-variation the Rayleigh cross section may easily fall below the Thomson value, the process hence being masked by scattering from free electrons (Burgess 1978*a*).

Other limitations on such bound-state scattering techniques (Burgess & Skinner 1974; Burgess 1978*a*; Burgess *et al.* 1980) stem from the temporal variation of the scattered light signal due to electron collisional processes even when the laser pulse is sustained. The rates are such that no major limitation occurs at tokamak densities ($n_e \lesssim 10^{20}\,\mathrm{m}^{-3}$), but for higher density plasmas the required laser power for saturation rises sharply and the duration of any significant laser-induced enhancement may drop to 10^{-10} s or less regardless of the incident laser pulse length. Again this problem would be partly alleviated if u.v. scattering from highly ionized species became possible, since collision rates associated with these more energetic transitions are much lower.

5. Highly charged ions in multi-kiloelectronvolt plasmas

Measurements of the spectral emission from highly ionized ions (net charge Z) are of interest to the plasma physicist in several contexts. In magnetic containment experiments, these ion concentrations can control the overall energy balance through ohmic heat and radiation loss terms, and redistribution of equilibrium-producing currents. In thermonuclear burn conditions

they may even prevent ignition (Summers & McWhirter 1979; Jensen *et al.* 1977). In laser compression experiments, elements located in different layers in the original target may end up emitting from the same plasma volume, and this can be vital evidence for instability mixing during the compression. In the context of this paper our chief interest in the high-Z ions is their role as diagnostic indicators. In low density tokamak plasmas, line intensities are important in ion diffusion studies while line shapes, particularly of forbidden lines, are often used for mass-motion and thermal-broadening measurements. In extreme pressure plasmas, Stark- and opacity-broadened lines may be interpreted in terms of the parameters $\int \rho \, dr$ and the density ρ.

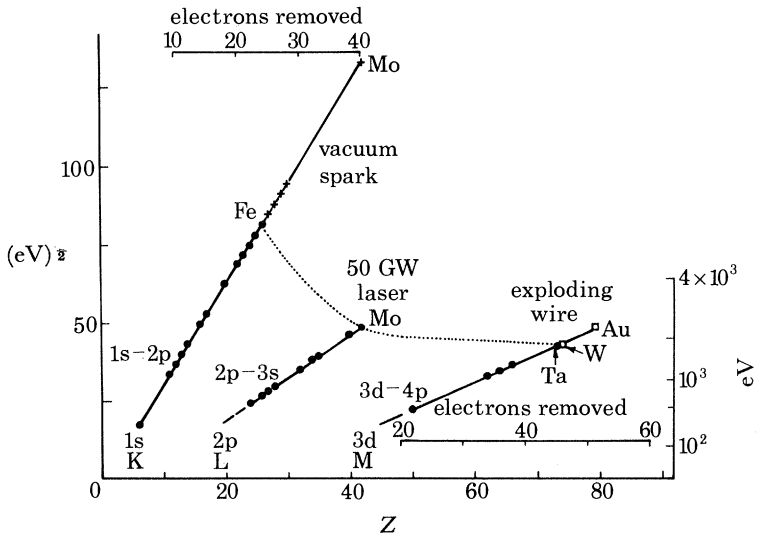

FIGURE 5. Semi-Moseley-plot of the ion species generated in various laboratory plasmas. ..., Upper boundary typically produced by laser irradiation of solid surfaces by using a focused ($F/1$) 50 GW beam of 1 ns duration. (Higher stages can be generated by more powerful lasers.)

5.1. *Equilibrium charge state of the plasma*

It follows from the elevated temperatures (more than 1 keV) and improved confinement ($n_e \tau \gtrsim 10^{18}$ m^{-3} s) in contemporary controlled fusion devices that impurity ions with charge stages $10 \lesssim Z \lesssim 50$ are to be expected. Further, the relative ion populations will be in stationary equilibrium, or nearly so (McWhirter 1975). The details will depend on the relative magnitude of the atomic rate processes and the diffusion rates, V_z; the variation in the ion charge z being given by

$$\frac{\partial N_z}{\partial t} + \frac{1}{r}\frac{\partial (r\Gamma_z)}{\partial r} = n_e[\alpha^{z-1}N^{z-1} + \beta^{z+1}N^{z+1} - (\alpha^z + \beta^z)\, N^z],$$

where α and β are the ionization and recombination rates and $\Gamma_z = D\partial N_z/\partial r = rV_z \partial N_z/\partial r$.

In tokamaks, the diffusion rates (Hirshman 1970) are often of the same order as the atomic rates (Summers 1974) so that one cannot *a priori* assume a completely stationary ionization–recombination balance.

The same general argument holds for the charge states in extreme pressureplasm as produced in laser irradiation experiments; in this case, however, the value of V_z is set by streaming mechanisms rather than diffusion.

Figure 5 shows a semi-Moseley-plot of the range of charge states observed in various plasma sources. The K-shell spectra of Mo has been recorded in a vacuum spark plasma by Beier &

Kunze (1978), while He-like Fexxv has been studied in the P.L.T. tokamak by Bitter *et al.* (1979*a*); charge states as high as Znxxix have been reported in laser-irradiated solid target experiments. In M-shell spectra, ions with charge states exceeding +50 have been observed in laser-irradiated targets and in the explosive deposition of the energy from electron beams

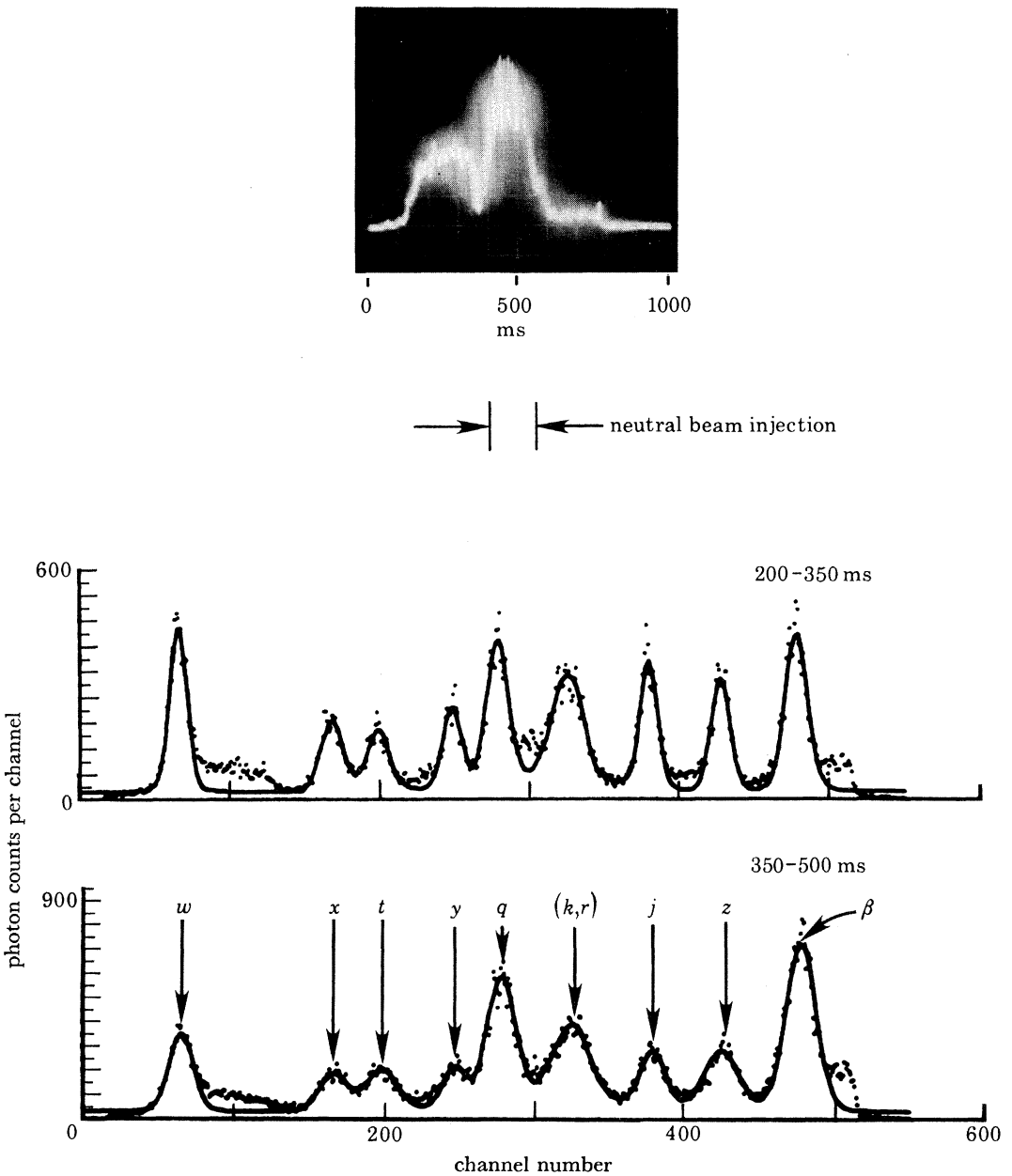

FIGURE 6. Upper insert shows the time-dependence of the spectrally integrated $1s^2$–$1s2p^1P_1$ Fexxv line '*w*' and its satellites before and during neutral H° beam injection into the P.L.T. tokamak. The total flux shows 'sawtooth' oscillations during the beam injection pulse. The change in the relative intensities I_q/I_W on beam injection indicates an increase of N(Fexxiv)/N(Fexxv) by a factor of 2, while the almost constant I_j/I_W ratio indicates little change in T_e (nomenclature as in Gabriel (1972)). These observations could be explained by charge exchange recombination $H^\circ + Fe^{24+} \rightarrow H^+ + Fe^{23+}$, or to enhanced transport of Fe^{24+} from the hot core during H° beam injection. (Courtesy of M. Bitter, Princeton Plasma Physics Laboratory.)

into fine wires. Beam foil target interactions, while not being plasmas, are capable of producing as competitively high ion stages as those in figure 5, provided that the ion projectiles have energies greater than about 10 MeV/u.

5.2. *X-ray spectroscopy of tokamaks*

A superb example of the information content to be derived from high resolution, $\lambda/\delta\lambda \approx 1.5 \times 10^4$, Bragg dispersion of the emission from a tokamak is shown in figure 6. The spectrum (Bitter *et al.* 1979*a*, *b*) shows the first allowed resonance line of Fexxv, '*w*', well resolved from its longer wavelength, $1s^2nl$–$1s2pnl$ ($n \gtrsim 2$), satellites and its associated forbidden and intercombination lines. By using the theoretical models developed by Gabriel and co-workers (Gabriel 1972; Bhalla *et al.* 1975) for the relative intensities of the satellites, T_e may be derived from the dielectronic satellites, and the ionization balance from the collisionally excited satellites. Departure of the observed relative ion populations from the calculated stationary ionization balance, calculated at T_e, may be interpreted (figure 6) in terms of ion diffusion rates (Bitter *et al.* 1979*a*). The detailed interpretation of the ion populations, however, depends crucially on having a thorough account of the plasma parameters $T_e(r, t)$, $n_e(r, t)$ and having confidence in the relevant atomic rate processes.

Finally, the resolution of the crystal spectrometer (Bitter *et al.* 1979*b*) is sufficiently high to unfold the thermal ion broadening and to demonstrate the increase in the ion temperature during H° beam injection. If the allowed resonance line '*w*' is used for such a purpose, figure 6, the higher satellite numbers ($1s2pnl$, $n > 2$) have to be subtracted from the intensity of the long wavelength wing.

5.3. *Forbidden lines in tokamaks*

Observations of and interest in forbidden lines of highly ionized atoms have until recently been confined to astrophysical plasmas (see, for example, Edlen 1969; Feldman *et al.* 1977). In tokamak plasmas, the parameters are similar to those of active solar regions so that forbidden lines in highly charged ions are now under study both theoretically (see, for example, Cowan 1977) and experimentally (see, for example, Bitter *et al.* 1979*a*; Mansfield *et al.* 1978). The former authors have observed the resonance decay of the $1s2s^3S_1$ metastable level in Fexxv in the X-ray region while the latter authors have studied the x.u.v. metastable levels associated with closed-shell configurations, for example, $3p^53d^{10}4s$ in Moxiv. The spontaneous decay rates of various allowed and forbidden transitions are compared in figure 7 with the collisional rates typical of tokamak plasma conditions. The dominance of the collisional rates over the A-values of forbidden lines at low transition energies would lead us to expect, on simple-minded considerations, that only those forbidden lines with $A \gtrsim 10^4\ s^{-1}$ and transition energies $\epsilon \gtrsim 10$ eV would be present in the tokamak spectrum. However, even lower energy transitions, particularly those within the $2s^n2p^m$ ground configurations of ionized metals, have been observed recently in tokamaks and studied by Suckewer & Hinnov (1978) and Suckewer *et al.* (1980*a*). The emission intensities of lines with A-values as low as 10^2–$10^4\ s^{-1}$, can be seen by inspection of the Tixiv, Tixviii emission from the DITE tokamak in figure 8. Since these $\Delta n = 0$ forbidden lines typically lie at long wavelengths in the v.u.v. and visible regions, their line profiles are useful monitors of ion temperature, as in the measurements on Fexx $2s^22p^3$, $^2D_{\frac{5}{2}-\frac{3}{2}}$ at 266.51 Å in the P.L.T. tokamak reported by Eubank *et al.* (1978).

Feldman *et al.* (1980) and Doschek & Feldman (1976) have outlined the diagnostic potential of these and similar $n = 2 \rightarrow 2$ line intensities for measuring T_e and n_e in tokamak plasmas. In

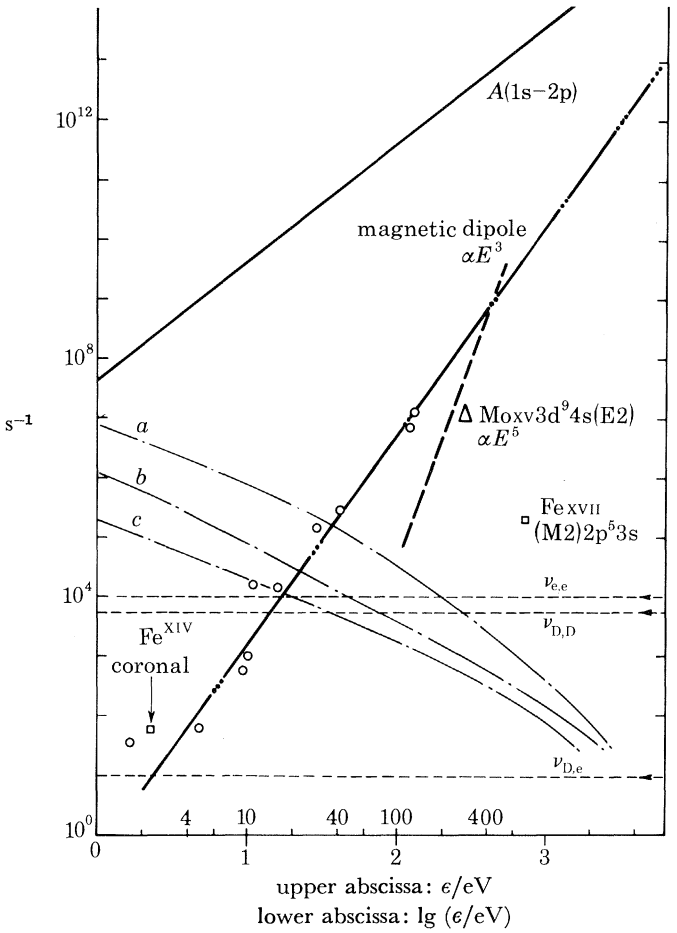

FIGURE 7. Spontaneous decay rates for various types of transitions (——, allowed 1s–2p; —·—, ○, magnetic dipole; □, magnetic quadrupole; – – –, △, electric quadrupole) against the transition energy ϵ/eV for $T_e = T_i = 1$ keV and $n_e = n_i = 10^{19}$ m^{-3}. The collisional decay rates $\langle\sigma v\rangle\, n_e$ (Lotz 1967) (a, $\langle\sigma v\rangle^{l}_{\mathrm{Lotz}}\, n_e$; b, $\langle\sigma v\rangle^{\mathrm{d.e.-e.x.}}_{i-k}\, n_e$; c, $\langle\sigma v\rangle^{\mathrm{e.x.}}_{i-k}\, n_e$) and thermalization rates ν_{ee}, $\nu_{D,e}$ and $\nu_{D,D}$ for typical tokamak conditions are plotted for comparison.

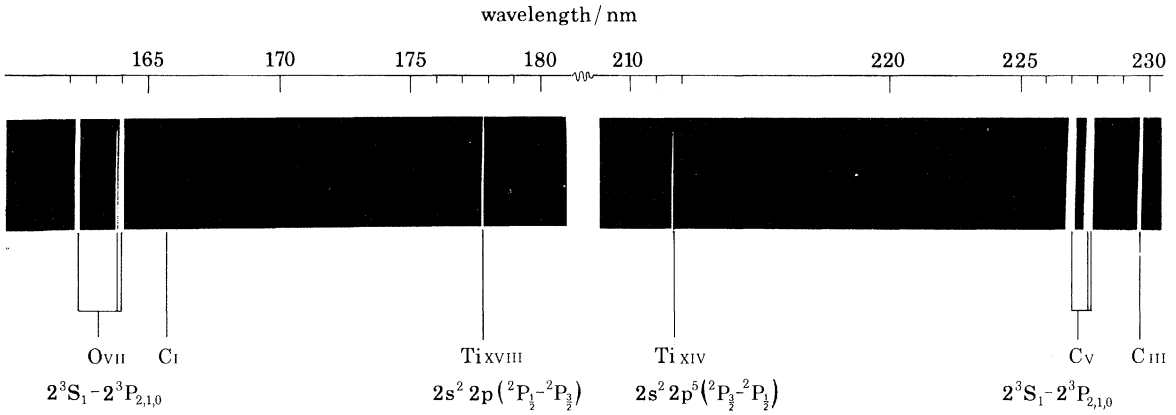

FIGURE 8. Forbidden transitions (spontaneous decay rate $A \approx 10^3$ s^{-1}) within the $1s^2 2p^n$ ground configuration of ionized titanium impurities in the DITE tokamak ($n_e \approx 2 \times 10^{19}$ m^{-3}, $T_e \approx 800$ eV). Reference emission lines from the $1s2s^3S_1$–$1s2p^3P_{2,1,0}$ triplets of oxygen and carbon impurities ($A \approx 10^8$ s^{-1} and $N(0) \approx 10 \times N(\mathrm{Ti})$) are seen to have intensities comparable with those of the metal lines.

these fusion devices, however, the electron parameters are likely to be measured to better than $\pm 20\%$ by other methods, so the main interest is likely to lie in the validity of model calculations of the line intensities, especially as a check on the atomic rate coefficients.

5.4. *Interpretation of emission line profiles in extreme pressure plasmas*

In low density plasma work Thomson-scattering and laser interferometric techniques have largely supplanted observations of pressure-broadened spectral line shapes as a primary density diagnostic. However, considerable interest in pressure-broadening processes has remained because of fundamental statistical mechanical problems and also because of secondary diagnostic applications, for example, in studying plasma turbulence (see, for example, Griem (1974) and Burgess (1978*b*) for references to the many publications in this field).

The continued academic interest in this area has recently had very important practical consequences in diagnostic applications to very dense (laser compressed) plasmas. These plasmas have core densities such that Thomson-scattering measurements would require the use of an x.u.v. laser. Despite current research on x.u.v. sources (Pert, this symposium), major breakthroughs will be necessary before laser diagnostics can be used on compressed plasmas. In the context of density diagnostics, observations of pressure-broadened X-ray lines from very dense plasmas offer a number of advantages over, say, relative line intensity measurements. Firstly, in a homogeneous optically thin plasma, line shapes depend only on local conditions and not on the spatial extent of the plasma.

In a spatially varying or optically thick plasma this advantage is not totally retained, but interpretation often remains more exact than with total line intensities. Second, pressure-broadened profiles are usually almost entirely density-dependent and very insensitive to electron temperature.

Against these advantages must be set the fact that line-shape predictions in very dense plasmas can be sensitive to many-body effects as yet little treated in detail (see, for example, Lee 1979; Lee *et al.* 1979; Burgess 1978*b*) and that higher spectral resolution is needed than for total emission intensity measurements. This latter requirement is significant in practice because, despite the high surface brightness, the resolution limits are set by the limited photon fluxes from the small, short-lived sources of laser compression plasmas. A further significance of line shape studies, that of radiation transport and the consequent effects on compressed plasma density, is outside the scope of this article.

Diagnostic applications of pressure-broadened line shapes rely totally on the accuracy of underlying theoretical predictions. The most important recent developments have concerned the separate but related effects of high density and high emitter charge (see Lee 1979; Burgess 1978*b*). At all densities the lines of most interest in diagnostic applications are affected to some extent by many perturber effects as well as by binary collision broadening. Theories developed originally for use in modest density plasmas (see, for example, Griem 1974) have been modified and used with some success at very high densities (for example, see Griem *et al.* 1979; Yaakobi *et al.* 1977, 1979). However, two separate considerations prejudice the applications of such theories at the highest density. The first is that as the mean interparticle separation, r_0, becomes comparable with the Debye length, λ_D, established treatments of properties such as the plasma dielectric function and the static microfield probability distribution become very dubious. As occur in the analogous case of metal physics, very high density approximations (when degeneracy effects limit the effective number of strongly interacting particles) are probably quite

good, but there is much less certainty about the important intermediate régime where the plasma is strongly interacting. This requires direct experimental study, preferably on more amenable plasmas than the very small short-lived ones generated in laser-compression experiments, and it is fortunate that parametrically similar conditions can be reached in much simpler sources (see, for example, Baker & Burgess 1979). The second, and very significant,

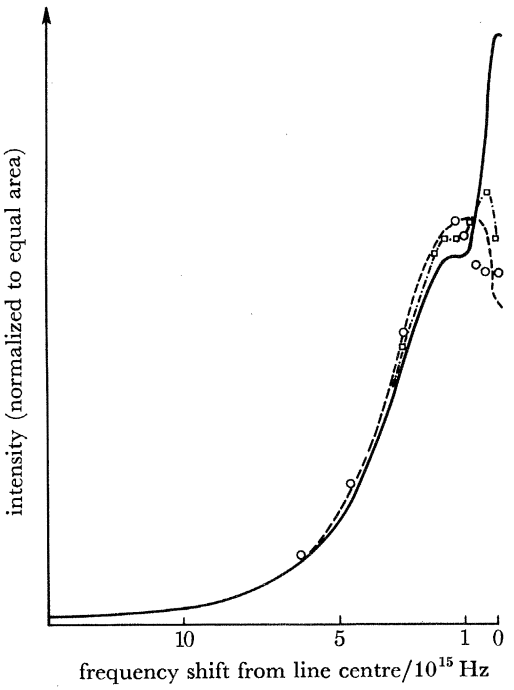

FIGURE 9. Computed line profiles of Lyman-γ ArXVIII including ion dynamics for various values of the mean charge state Z of the perturber ions for $T_e = 450$ eV and $n_e = 3 \times 10^{29}$ m^{-3}. Increasing Z from one to fifteen lowers the peak intensity by *ca.* 40% and broadens the profile. The profiles □—·—□ and ○——○ correspond to a mean Z of 9.3, the former being due to a fictitious single chemical species and the latter due to a mixture of $Z = 1$ (——) and $Z = 15$ (— — —). Purely static ion model calculations show only a weak dependence on Z and give a central intensity that is a factor of *ca.* 1.5 higher (with a consequently narrower profile) than the full curve corresponding to the dynamic calculations for $Z = 1$.

problem is the local polarization of the surrounding plasma by high-charge state emitters. The marked effects that this can cause on spectral line shapes and shifts have been demonstrated in a series of computations by Lee (1979). A separate consequence of high emitter charge at high density, the suppression of Doppler broadening due to the very short emitter mean free path, while not yet observed, should be rather common in laser-generated plasmas (Burgess *et al.* 1979). Finally, ion-dynamic effects, originally discovered in low density plasmas (Burgess 1970; Mahon *et al.* 1973; Wiese *et al.* 1975) turn out to be very significant for high-Z emitters in very dense plasmas where substantial modifications to line widths and hence deduced densities can result (see figure 9, and Lee & Freeman (1980)).

Experimentally, numerous applications of line-shape measurements to diagnostics of dense plasmas have been made, and some of these have been discussed in recent reviews by both authors of this paper (Peacock 1977; Burgess 1978*b*). The most important criterion in such work is discrimination against optical opacity effects by the simultaneous study of several

line-profiles, for example, along a spectral series, in which case a unique fit can often be made to the spatial structure of the plasma as well as to the absolute value of the density (see, for example, Kilkenny *et al.* 1980; Yaakobi *et al.* 1979).

6. Basic physics problems related to diagnostic developments

One of the important changes with the new generation of fusion devices is that for the first time laboratory conditions and parameters such as plasma density and charge state have substantially outrun those commonly encountered in astronomical observation (although not of course those, in stellar interiors, supernovae, etc.). Many authors (for example, Weise 1978) have referred to the serious shortage of atomic data appropriate to the study of highly charged ions ($15 \gtrsim Z \gtrsim 50$) in laboratory plasmas. Atomic structure data such as transition probabilities, particularly forbidden and intersystem line strengths, fine structure interactions, e.g. relativistic and Lamb shifts, need to be assessed for such high-z ions. Even orthodox binary collisional processes such as excitation, ionization and recombination have mostly been calculated for lower ion stages and for astrophysical plasmas. Such data need extention to cover current laboratory plasma conditions. In addition, the laboratory studies emphasize a set of quite new 'priorities'. The problem of charge-transfer recombination in particle beam heated tokamaks is but one example. Theoretical charge transfer cross sections do exist (see, for example, Olson & Salop 1976, 1977; Olson *et al.* 1978; Gorzdanov & Janev 1978; Ryufuku & Watanabe 1978) but discrepancies of the order of two in the calculations make a significant difference to the interpretation of the overall energy balance (Krupin *et al.* 1979; Suckewer *et al.* 1980*b*). Charge-exchange processes will also play a significant part in the interpretation of laser fluorescence experiments at high temperatures, although largely ignored in theoretical models to date (Koopman *et al.* 1978).

Experimentally, the long-lived conditions in tokamaks offer unique possibilities for spectroscopic studies involving high-Z ions. Some preliminary work has already been done on basic collision processes (see, for example, Breton *et al.* 1978) but there is a strong case for a tokamak facility at least partly devoted to fundamental physics such as atomic structure and for the development of diagnostic techniques, e.g. fluorescence spectroscopy, magnetic field measurements, the detailed interpretation of f.i.r. emission and lastly for active diagnostics such as the technique used by Afrosimov *et al.* (1978) for measuring high-Z impurity concentrations by means of charge transfer from H° beam probes.

The least explored aspects of emission from high-Z ions occur in high density plasmas when the interparticle distance is of the same order or larger than the Debye length. Local polarization of the plasma due to the presence of the highly charged emitter can control not only the many-body effects contributing to line shapes as discussed in §5.4, but also the collisional rates controlling level populations etc. which are normally considered as purely binary processes. In the context of line-shape work, it has long been recognized that local polarization effects could play an important role (Grieg *et al.* 1970; Burgess 1972), although because of the complexity of the underlying theoretical problem there has been considerable controversy about various results (Grieg *et al.* 1970; Burgess & Peacock 1971; Burgess 1972; Volonte 1978). In perhaps the most thorough quantum statistical analysis to date Lee (1979) and Lee & Freeman (1980) have shown for high-Z emitters that marked effects can occur both in line shifts and asymmetries, and in producing new structures due to ion sound waves, which, (§5.4), offer diagnostic

possibilities in determining the plasma charge state. For excitation and ionization rates etc., the standard argument has been that a purely binary collision approximation is valid until very high densities ($n_e > 10^{31}$ m^{-3}) (Vinogradov *et al.* 1974). However, Burgess (1978*b*) has pointed out that these arguments neglect the effects of the long range Coulomb interaction on the near-threshold behaviour of the cross sections, usually of dominant importance, and that in consequence many-body corrections may occur even for relatively low charge state emitters, such as Nex in plasma with densities as low as $n_e = 10^{28}$ m^{-3}.

Some aspects of these problems can be studied in relatively low temperature laboratory plasmas (Baker & Burgess 1978; Finken *et al.* 1978) such as the *z*-pinch where the condition $r_0 \approx \lambda_D$ can be reached. In extreme pressure plasmas such as are produced by laser compression, detailed quantitative study is still limited by purely experimental constraints on spatial, time and spectral resolution. While many important fundamental problems concerning high-*Z*-emitters will require such laser compressed plasmas for study, developments are still required in the experimentalist's art, for instance in generating plasmas with high reproducibility to overcome photon flux limitations.

References (Peacock & Burgess)

Afrosimov, V. V., Gordeev, Yu. S., Zinovev, A. N. & Korotkov, A. A. 1978 *Pis'ma Zh. Eksp. Teor Fiz.* **28**, 541–543.

Ahlstrom, H. G., Coleman, L. W., Rienecker, F. & Slivinsky, V. W. 1978 *J. opt. Soc. Am.* **68**, 1731–1741.

Attwood, D. T. 1978 *IEEE J. Quantum Electron.* **14**, 909–923.

Attwood, D. T., Ceglio, N. M., Campbell, E. M., Larsen, J. T., Mathews, D. M. & Lane, S. L. 1979 Lawrence Livermore Laboratory Preprint, UCRL-83541.

Baker, E. A. M. & Burgess, D. D. 1979 *J. Phys.* B **12**, 2097–2113.

Beier, R. & Kunze, J. H. 1978 *Z. Phys.* A **285**, 347–352.

Bhalla, C. P., Gabriel, A. H. & Presnyakov, L. P. 1975 *Mon. Not. R. astr. Soc.* **172**, 359–375.

Bitter, M., Hill, K. W., Sauthoff, N. R., Efthimion, P. C., Meservey, E., Roney, W., Von Goeler, S., Horton, R., Goldman, M. & Stodiek, W. 1979*a* *Phys. Rev. Lett.* **43**, 129–132.

Bitter, M., Von Goeler, S., Horton, R., Goldman, M., Hill, K. W., Sauthoff, N. R. & Stodiek, W. 1979*b* *Phys. Rev. Lett.* **42**, 304–307.

Bogen, P. & Hintz, E. 1978 *Comments Plasma Phys. Controlled Fus.* **4**, 115–130.

Bol, K., Aranasalam, V., Bitter, M. *et al.* 1979 *Nucl. Fus. Suppl.* **1**, 11–32.

Breton, C., De Michelis, C., Finkenthal, M. & Mattioli, M. 1978 *Phys. Rev. Lett.* **41**, 110–113.

Burakov, V. S., Misyakov, P. Ya., Naumenko, P. A., Nechaev, S. V., Razdobarin, G. T., Semenov, L. V., Sokolova, L. V. & Folomkin, I. P. 1977 *JETP Lett.* **26**, 403–406.

Burgess, D. D. 1970 *J. Phys.* B **3**, L70–74.

Burgess, D. D. & Peacock, N. J. 1971 *J. Phys.* B **4**, L94–97.

Burgess, D. D. 1972 *Space Sci. Rev.* **13**, 493–527.

Burgess, D. D. & Skinner, C. H. 1974 *J. Phys.* B **7**, L297–301.

Burgess, D. D. 1978*a* In *Physics of ionized gases*, pp. 543–577. Belgrade: Institute of Physics. Also available as *U.K.A.E.A. Culham Laboratory Report* CLM P-568.

Burgess, D. D. 1978*b* In *Physics of ionized gases*, pp. 501–541. Belgrade: Institute of Physics; also available as U.K.A.E.A. Culham Laboratory Report CLM P-567.

Burgess, D. D., Kolbe, G. & Ward, J. M. 1978 *J. Phys.* B **11**, 2765–2778.

Burgess, D. D., Everett, D. & Lee, R. W. 1979 *J. Phys.* B **12**, L755–758.

Burgess, D. D., Myerscough, V. P., Skinner, C. H. & Ward, J. M. 1980 *J. Phys.* B **13**, 1675–1701.

Burgess, A., Summers, H. P., Cochrane, D. M. & McWhirter, R. W. P. 1977 *Mon. Not. R. astr. Soc.* **179**, 275–292.

Burrell, C. F. & Kunze, H. J. 1972 *Phys. Rev. Lett.* **28**, 1–4.

Ceglio, N. M., Attwood, D. T. & George, E. V. 1977*b* *J. appl. Phys.* **48**, 1566–1569.

Ceglio, N. M. & Coleman, L. W. 1977*a* *Phys. Rev. Lett.* **39**, 20–24.

Ceglio, N. M. & Smith, H. I. 1978 *Rev. scient. Instrum.* **49**, 15–20.

Chamberlain, J., Costley, A. E. & Burgess, D. D. 1971 *Proceedings of the Conference on Submillimetre Waves*, p. 573. Brooklyn Institute of Technology.

PHILOSOPHICAL TRANSACTIONS OF THE ROYAL SOCIETY A MATHEMATICAL, PHYSICAL & ENGINEERING SCIENCES

Costley, A. E. 1979 *Trends in physics*, ch. 5, pp. 351–360. Bristol: Adam Hilger Ltd.
Costley, A. E., Hastie, R. J., Paul, J. W. M. & Chamberlain, J. 1974 *Phys. Rev. Lett.* **33**, 758–761.
Costley, A. E. & T.F.R. Group 1977 *Phys. Rev. Lett.* **38**, 1477–1480.
Cotter, D. 1979 *Optics Commun.* **31**, 397–400.
Cowan, R. D. 1977 *Los Alamos Laboratory Report*. LA-6679-MS.
Dimmock, D., Hinnov, E. & Johnson, L. C. 1969 *Physics Fluids* **12**, 1730–1732.
Doschek, G. A. & Feldman, U. 1976 *J. appl. Phys.* **47**, 3083–3087.
Equipe T.F.R. 1978 *Nucl. Fus.* **18**, 647–731.
Edlen, B. 1969 *Solar Phys.* **9**, 439–445.
Eubank, H., Goldston, R. J. *et al.* 1979 *Nucl. Fus. Suppl.* **1**, 167–197.
Eubank, A. & Sindoni, E. (ed.) 1975 *Plasma diagnostics and data acquisition systems*. Proceedings of course held by International School of Plasma Physics, Varenna, Italy (1975). Milan: C.N.R.–Euratom Plasma Physics Laboratory.
Evans, D. E. 1976*a* *Physica*. **82**, 27–42.
Evans, D. E. 1976*b* In *Physics of ionized gases*, pp. 641–666. Yugoslavia: University of Ljubljana.
Evans, D. E. 1977 *Culham Laboratory Report* CLM-P482.
Evans, D. E. & Carolan, P. G. 1970 *Phys. Rev. Lett.* **25**, 1605–1608.
Evans, D. E. & Katzenstein, J. 1969 *Rep. Prog. Phys.* **32**, 207–271.
Feldman, U., Doschek, G. A., Chung-Chieh Cheng & Bhatia, A. K. 1980 *J. appl. Phys.* **51**, 190–201.
Feldman, U., Doschek, G. A. & Rosenberg, F. D. 1977 *Astrophys. J.* **215**, 65–665.
Finken, K. H., Bertschinger, G., Maurmann, S. & Kunze, H. J. 1978 *J. quant. Spectrosc. radiat. Transfer*. **20**, 467–476.
Forrest, M. J., Carolan, P. G. & Peacock, N. J. 1978 *Nature, Lond.* **271**, 718–722.
Freund, H. P., Wu, C. S., Lee, L. C. & Dillenburg, D. 1978 *Physics. Fluids*. **21**, 1502–1508.
Gabriel, A. H. 1972 *Mon. Not. R. astr. Soc.* **160**, 99–199.
Gorzdanov, T. P. & Janev, R. K. 1978 *Phys. Rev.* A **17**, 880–896.
Grieg, J. A. R., Griem, H. R., Jones, L. A. & Oda, T. 1970 *Phys. Rev. Lett.* **24**, 3–5.
Griem, H. R. 1974 *Spectral line broadening in plasmas*. New York: Academic Press.
Griem, H. R., Blaha, M. & Kepple, P. C. 1979 *Phys. Rev.* **19**, 2421–2432.
Himmel, G. & Pinnekamp, F. 1977 *J. Phys.* B **10**, 1457–1464.
Hirshman, S. P. 1970 *Physics Fluids* **19**, 155–158.
Hutchinson, I. H., Molvig, K. & Yuen, S. Y. 1978 *Phys. Rev. Lett.* **40**, 1091–1094.
Jenson, R. V., Post, D. E., Grasberger, W. H., Tarter, C. B. & Lokke, W. A. 1977 *Nucl. Fus.* **17**, 1187–1196.
Kilkenny, J. D., Lee, R. W., Key, M. H. & Lunney, J. G. 1980 Submitted to *Phys. Rev.*
Koopman, D. W., McIlrath, T. J. & Myerscough, V. P. 1978 *J. quant. Spectrosc. radiat. Transfer*. **19**, 555–567.
Krupin, V. A., Marchenko, V. S. & Yakovlenko, S. T. 1979 *Pis'ma Zh. Eksp. Teor. Fiz*. **29**, 353–357.
Luhmann, N. C. 1979 *Instrumentation and techniques for plasma diagnostics – an overview in infra-red and submillimeter waves* (ed. K. Button). London: Academic Press.
Lotz, W. 1967 *Astrophys. J. Suppl.* **14**, 207–238.
Lee, R. W. 1979 *J. Phys.* B **12**, 1145–1163.
Lee, R. W., Bromage, G. & Richards, A. G. 1979*b* *J. Phys.* B **12**, 3445–3453.
Lee, R. W. & Freeman, A. J. 1980 *J. quant. Spectrosc. radiat. Transfer*. (In the press.)
Mahon, R., McIlrath, T. J. & Koopman, D. W. 1978 *Appl. Phys. Lett.* **33**, 305–307.
Mahon, R., Lee, R. W. & Burgess, D. D. 1973 *J. Phys.* B **6**, 354–363.
Mansfield, M. W. D., Peacock, N. J., Smith, C. C., Hobby, M. G. & Cowan, R. D. 1978 *J. Phys.* B **11**, 1521–1544.
McWhirter, R. W. P. 1975 In *Course on Plasma Diagnostics and Data Acquisition Systems*, Proceedings, International School of Plasma Physics, Varenna, Italy (ed. A. Eubank & E. Sindoni). Milan: C.N.R.–Euratom Plasma Physics Laboratory.
Measures, R. M. 1968 *J. appl. Phys.* **39**, 5232–5245.
Muller, C. H. & Burrell, K. H. 1980 Submitted to *Phys. Rev. Lett.*; see also General Atomic preprint GA-A15806, General Atomic, San Diego (1980).
Olson, R. E., Berkner, K. H., Graham, W. G., Pyle, R. V., Schlachter, A. S. & Stearns, J. W. 1978 *Phys. Rev. Lett.* **41**, 163–166.
Olson, R. E. & Salop, A. 1977 *Phys. Rev.* A **16**, 531–541.
Olson, R. E. & Salop, A. 1976 *Phys. Rev.* A **14**, 579–585.
Peacock, N. J. 1978 *Proc. XIIIth Conf. on Phenomena in Ionised Gases, 1977*, Berlin, G.D.R., vol. – Invited lectures, pp. 385–405. Phys. Soc. of G.D.R.
Razdobarin, G. T. & Fotomkin, I. P. 1979 *Diagnostics for fusion experiments*. Proc. Int. School of Plasma Physics, Varenna, Italy, Sep. 1978 (ed. E. Sindoni & C. Wharton), pp. 311–325. Oxford: Pergamon Press.
Reintjes, J. 1979 *Optics Lett.* **4**, 242–244.
Ryufuku, H. & Watanabe, T. 1978 *Phys. Rev.* A **18**, 2005–2015.
Sauthoff, N. R., Von Goeler, S. & Stodiek, W. 1978 *Nucl. Fus.* **18**, 1445–1458.

PHILOSOPHICAL TRANSACTIONS OF THE ROYAL SOCIETY A MATHEMATICAL, PHYSICAL & ENGINEERING SCIENCES

Schweer, B., Rusbuldt, D., Hintz, E., Roberts, J. B. & Husimsky. Paper presented to 4th International Conference on Plasma Surface Interactions in Controlled Fusion Devices, 21–25 April 1980, Garmisch-Partenkirchen, F.D.R.

Sheffield, J. 1975 *Plasma scattering of electromagnetic radiation*. New York: Academic Press.

Sindoni, E. & Wharton, C. (ed.) 1979 *Diagnostics for fusion experiments*. Proceedings of course held by International School of Plasma Physics, Varenna, Italy (1978). Oxford: Pergamon Press.

Slusher, R. E. & Surko, C. M. 1980 *Physics. Fluids*. **23**, 472–490.

Suckewer, S., Fonck, R. & Hinnov, E. 1980*a* *Phys. Rev.* A **21**, 924–927.

Suckewer, S. & Hinnov, E. 1978 *Phys. Rev. Lett.* **41**, 756–759.

Suckewer, S., Hinnov, E., Bitter, M., Hulse, R. & Post, D. 1980*b* *Phys. Rev.* A **22**, 725–731.

Summers, H. P. 1974 *Appleton Laboratory Report* IM367.

Summers, H. P. & McWhirter, R. W. P. 1979 *J. Phys.* B **12**, 2387–2412.

Vinogradov, A. V., Sobelman, I. I. & Yukov, E. A. 1974 *Soviet J. Quantum Electron.* **1**, 268.

Volonte, S. 1978 *J. Phys.* D **11**, 1615–1638.

Wiese, W. L., Kelleher, D. E. & Helbig, V. 1975 *Phys. Rev.* A **11**, 1854–1864.

Wiese, W. L. 1978 *Physics of Ionized Gases*, pp. 661–696. Belgrade: Institute of Physics.

Wrobel, W. G., Steuer, K. H. & Rohr, H. 1976 *Phys. Rev. Lett.* **37**, 1218–1221.

Yaakobi, B., Steel, D., Thorsos, E., Hauer, A. & Perry, B. 1977 *Phys. Rev. Lett.* **39**, 1526–1529.

Yaakobi, B., Steel, D., Thorsos, E., Hauer, A., Perry, B., Skupsky, S., Geiger, J., Lee, C. M., Letzring, S., Rizzo, J., Mukaiyama, J., Lazarus, E., Halpern, G., Deckman, H., Delettrez, J., Soures, J. & McCrory, R. 1979 *Phys. Rev.* A **19**, 1247–1262.

PHILOSOPHICAL TRANSACTIONS OF THE ROYAL SOCIETY A MATHEMATICAL, PHYSICAL & ENGINEERING SCIENCES

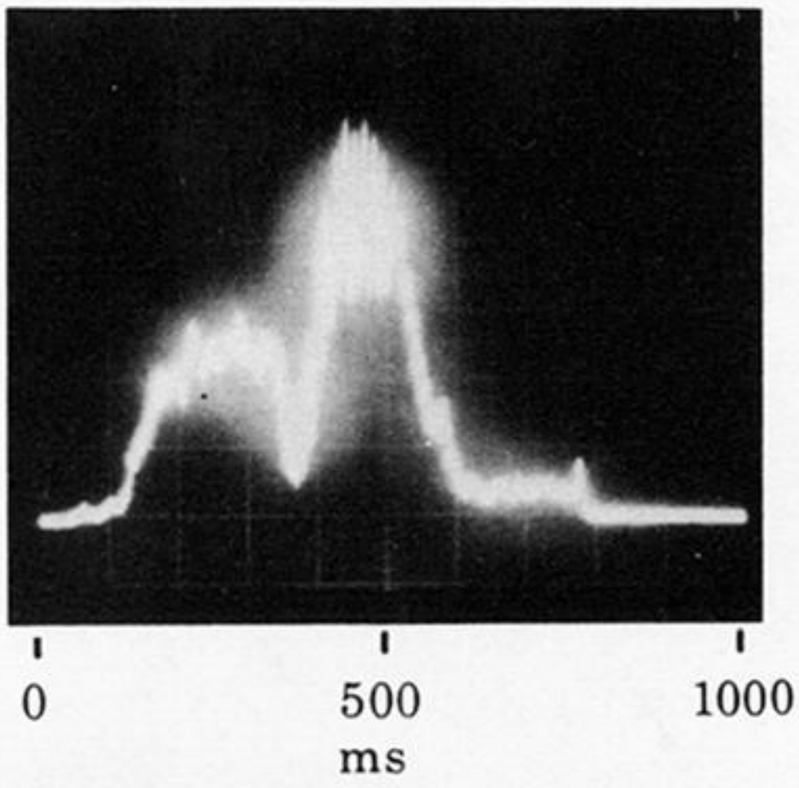

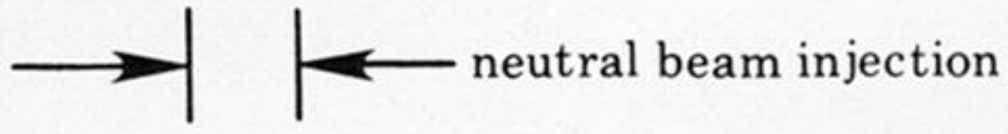

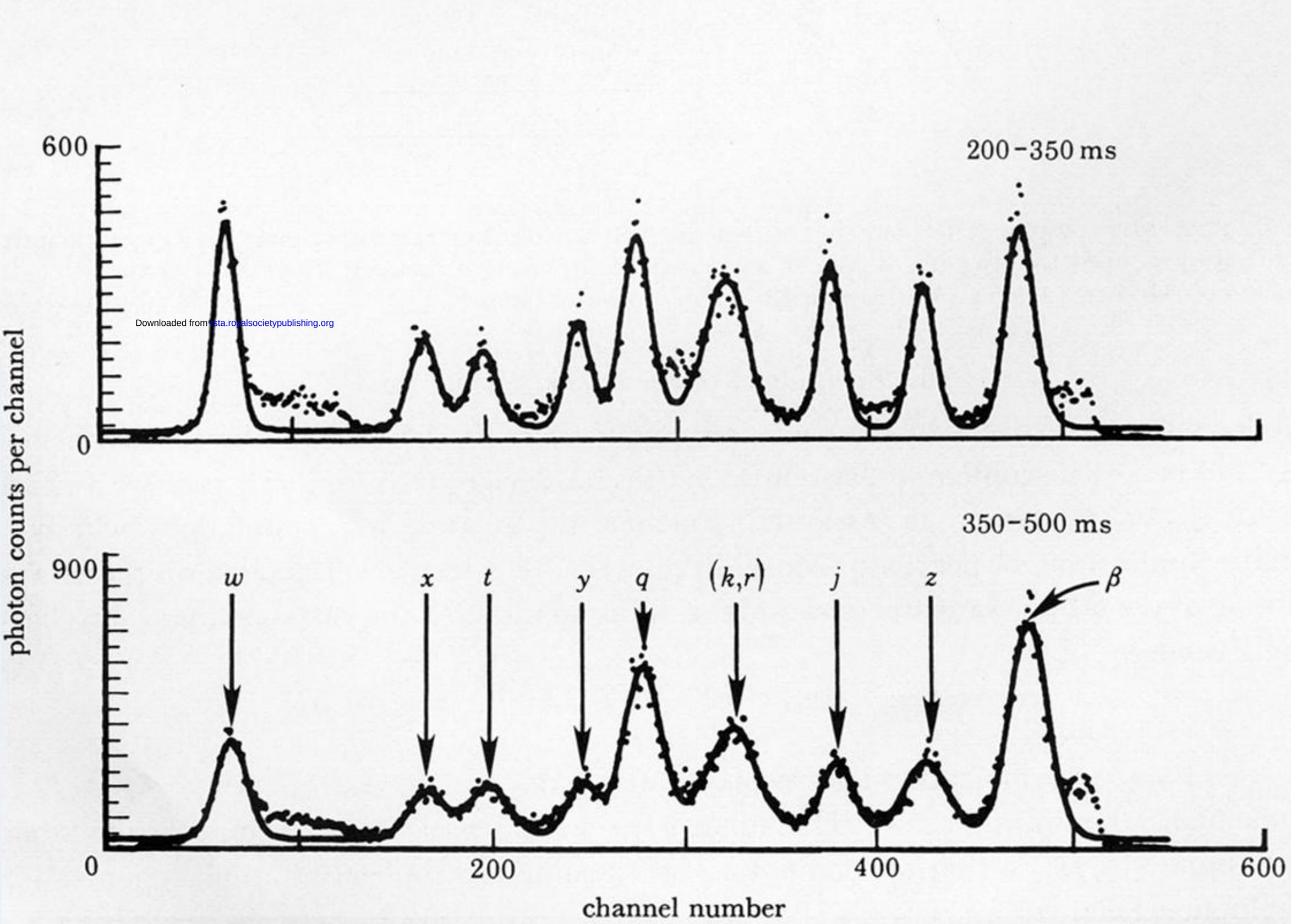

FIGURE 6. Upper insert shows the time-dependence of the spectrally integrated $1s^2$–$1s2p^1P_1$ Fexxv line 'w' and its satellites before and during neutral H° beam injection into the P.L.T. tokamak. The total flux shows 'sawtooth' oscillations during the beam injection pulse. The change in the relative intensities I_q/I_W on beam injection indicates an increase of N(Fexxiv)/N(Fexxv) by a factor of 2, while the almost constant I_j/I_W ratio indicates little change in T_e (nomenclature as in Gabriel (1972)). These observations could be explained by charge exchange recombination $H^\circ + Fe^{24+} \rightarrow H^+ + Fe^{23+}$, or to enhanced transport of Fe^{24+} from the hot core during H° beam injection. (Courtesy of M. Bitter, Princeton Plasma Physics Laboratory.)